Ligand and Solvent Effects on the Catalytic Activity and Lifetime of Zwitterionic Nickel(II) Catalysts for Alternating CO-Ethylene Copolymerization

Linhui Zhu,[a] Yiwei Dai,[a] Briana R. Schrage,[b] Christopher J. Ziegler,[b] and Li Jia,[a,b*]

[a] School of Polymer Science and Polymer Engineering, The University of Akron, Akron, OH 44325-3909, USA
[b] Department of Chemistry, The University of Akron, Akron, OH 44325-3601, USA

* Correspondence should be sent to: ljia@uakron.edu

Abstract

A series of zwitterionic nickel(II) compounds with anionic diphosphine ligands having varied substituents have been synthesized and studied as catalysts for CO-ethylene copolymerization. The electron-donating abilities of the ligands are assessed on the basis of the infrared absorptions of the CO-stretching vibrations of their Ni(0) carbonyl compounds. The equilibriums between Ni(II)-methyl and Ni(II)-acetyl and 4-coordinate and 5-coordinate Ni(II)-acetyls are studied using NMR and IR spectroscopies. With respect to the catalytic performances, a certain degree of steric hindrance around the Ni(II) center is required to achieve a high polymerization activity. The steric hindrance likely disfavors the 5-coordinate catalytically dormant state. Further increased steric congestion decreases the catalytic activity. The electron-donating ability of the ligand on the catalytic activity is modest within the relatively narrow range of variation of the present study. The catalyst lifetime and overall productivity are markedly improved by the presence of the *o*-methoxy ancillary on the phenyl group of the ligand although the *o*-methoxy decreases the activity of the catalyst. A comparison of the *o*-methoxy- and *o*-methyl-substituted ligands attributes the stabilization to the coordinating ability of the *o*-methoxy group rather than a steric or inductive electronic origin. The present catalysts are several times faster and more productive in THF than in toluene at room temperature. The increased activity is attributable to the coordinating ability of THF as opposed to polarity. The polymer products are strictly alternating copolymers of CO and ethylene.

Introduction

Transition metal-catalyzed alternating copolymerization of olefins and carbon monoxide (CO) has continuously attracted scientific interests since its discovery.[1-4] The wide range of potential applications of the aliphatic polyketone products, the low cost of CO and olefins, and the low carbon footprint of CO are practical motivations to study this type of polymerization.[5] The photodegradability of the ketone structure further provides an incentive stemmed from the recent emphasis on environmental degradability of plastics.[6]

Cationic Pd(II) catalysts with bidentate phosphine ligands are highly active and highly productive for the alternating copolymerization, with the activity of the catalyst systems in commercial applications reaching ~6000 g of polyketone/ (g of Pd)$^{-1}$ h^{-1} and the overall productivity ~10^{6} g of polyketone/g of Pd.[3, 7] In this paper as the units indicate, "activity" refers to the amount of product produced per unit time by a unit amount of catalyst, and "productivity" refers to the amount of product produced in a given amount of time by an unit amount of catalyst. The activities of the Ni(II) analogs of the cationic Pd catalysts are also very high at least when certain diphosphine ligands are used.[8-11] However, they are less productive than their Pd counterparts by several orders of magnitude. Neutral Ni(II) catalysts have also been investigated.[12-15] Their productivities are also orders of magnitude lower than the cationic Pd catalysts. The Pd catalysts are also capable of non-alternating CO-ethylene copolymerization,[16-24] while the Ni analogs are not.

We became interested in zwitterionic nickel compounds bearing an anionic diphosphine ligand [25-37] as the catalysts for CO-ethylene alternating copolymerization initially to improve the activity but later the productivity after we realized that the productivity, not the activity, was the problem of the Ni catalysts.[38, 39] The rationale is that the electrostatic attraction between the anionic ligand and the cationic metal center provides additional stability to the metal complex, in particular in the case of carbonylation against ligand substitution by CO, in comparison to the cationic analogs. Here, we provide a full account of our attempt of improving the productivity by systematically varying the substituents on the anionic phosphine framework (Figure 1) and the electronic and steric effects of the ligand on the activity and overall productivity of the catalyst.

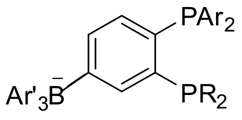

a – f

	Ar	R	Ar'
a	Ph	^{i}Pr	3,4-difluorophenyl
b	*o*-methoxyphenyl	Ph	3,4-difluorophenyl
c	*o*-methoxyphenyl	^{i}Pr	3,4-difluorophenyl
d	*o*-methoxyphenyl	Et	3,4-difluorophenyl
e	*o*-methoxyphenyl	Ph	*o*-tolyl
f	*o*-tolyl	^{i}Pr	3,4-difluorophenyl

Figure 1. Structure of anionic phosphine ligands explored in this work.

Results and discussion

Synthesis of Ligands and Nickel Complexes

The general synthetic route for the anionic ligands and the nickel compounds is shown in Scheme 1. Lithiation of **1g** – **1i** at -78 °C in Et_2O followed by addition of the corresponding phosphine chloride gives **2j** – **2n**. Lithiation in THF followed by addition of the triarylborane converts **2j** – **2n** to the lithium salts of the anionic ligands, **3a** – **3f**. Reaction of **3a** – **3f** with

$Ni(COD)_2$ under 1 atm of CO at room temperature affords the Ni(0) compounds, **4a – 4f**. Zwitterionic Ni(II) acetyl compounds, **5a – 5f**, are synthesized in high yields by reaction of **4a – 4f** with $Me_3O^+BF_4^-$ under CO. All compounds are characterized by standard spectroscopic techniques.

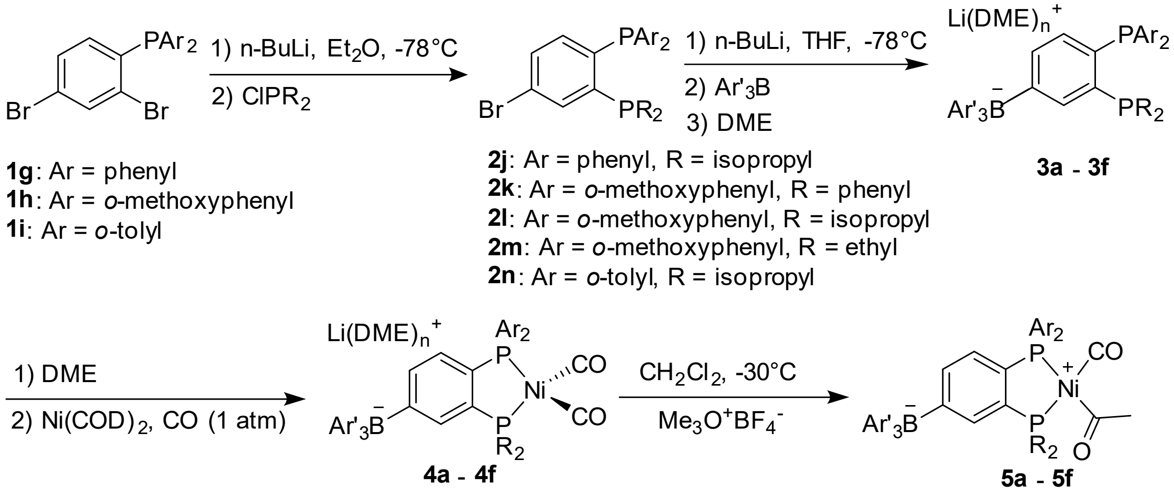

Scheme 1. General synthetic route for anionic phosphines and nickel compounds. Suffices **a** - **f** designate the ligand as indicated in Figure 1.

A few things are noteworthy regarding the choices of the borate anion and the synthetic method. For the borate, we have previously reported that the borate with Ar' = Ph decomposes due to its susceptible to electrophilic attack when the Ni(II) alkyl or hydride is exposed to CO.[38] The attempts of forming the borate using tris(pentafluorophenyl)borane failed because of aryl-redistribution. Tris(3,4-difluorophenyl)borane is used here as a compromise that gives enough stability to the borate in **a** – **d** and **f** when the Ni(II) complexes are exposed to CO and avoids aryl-redistribution during synthesis of the ligands.[39] By including ligand **e** with Ar' = *o*-tolyl, we test the possibility of sterically shielding the borate from electrophilic attack. For isolation of the Ni(II) acetyl compounds or any Ni(II) alkyls, allyls, or hydrides, we explored various routes using Ni(II) dihalides, allyl-Ni(II) halides, or Ni(II) diacetoacetate as the source of Ni. The method shown in Scheme 1 is superior to the others. For example, no attempt succeeded in isolating **4a** or its hydride, allyl, or alkyl analogs using the aforementioned starting materials. An allylic derivative of **4a** was isolated by reaction of the protonated ligand with $Ni(COD)_2$.[39] The geometries of the acetyl and CO relative to the unsymmetric diphosphine in **5a** – **5f** are assigned according to single-crystal X-ray diffractions of representative members, **5b** and **5d**. No geometric isomers of **5a** – **5f** are observable in solution by ^{1}H NMR.

Crystal structures of Ni(II) compounds

The X-ray crystallographic structure of **5b** was previously reported.[40] For this report, we obtained two crystal structures. Compound **5d** and its five-coordinate derivative, **5d**•CO, co-crystallize in the solid state. We have also obtained a second structure of the five-coordinate derivative, **5d**•CO, which crystalized by itself. Their X-ray structures are shown in Figure 2. The 4-coordinate **5d** adopts a square planar structure as seen in **5b**. The more electron-donating side of the bidentate phosphine PEt_2 is *trans* to CO as in **5b**. The 5-coordinate **5d**•CO adopts a distorted trigonal bipyramidal geometry, and the conformation of this molecule is identical in both crystal forms. Two COs and -PEt_2 are in the equatorial plane, and the acetyl and the other phosphine are in the axial positions. The axial ligands are slightly bent with a bond angle of 171.07(11)°. All Ni-ligand bond distances in the 5-coordinate **5d**•CO are elongated somewhat in comparison to the corresponding distances in the 4-coordinate **5d**. The C-O distances in the CO ligands of **5d**•CO (1.133(4) and 1.152(5) Å) are somewhat longer than that in the 4-coordinate **5d** (1.081(12) Å), indicating that back-donation from Ni to the antibonding π^* orbital of CO is stronger in **5d**•CO than in **5d**. The differences between the C-O distances of the acetyls (1.211(4) vs 1.218(17) Å) and the acetyl C-Ni distances (1.993(4) and 1.98(2) Å) in **5d**•CO and **5d** are statistically insignificant. The distances between O atoms of the methoxy groups and the Ni center in all three structures are far beyond the typical bonding distance.

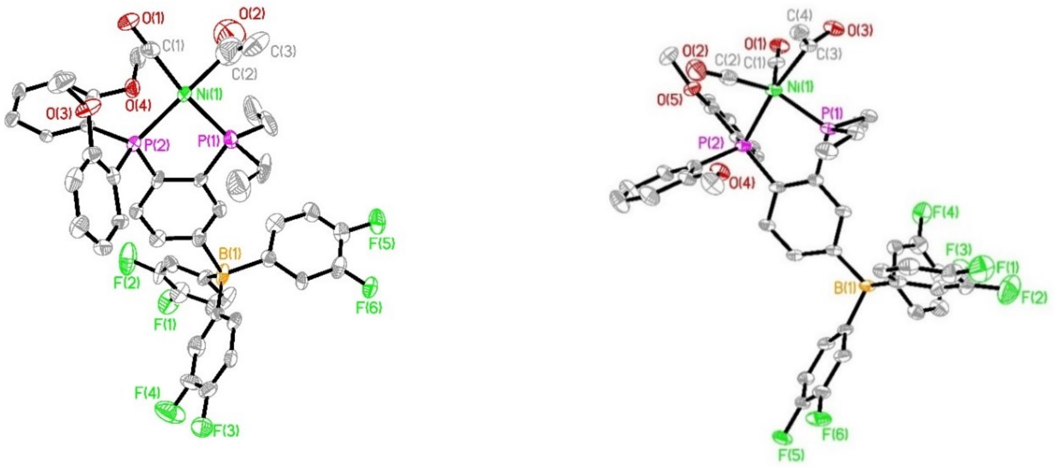

Figure 2. Crystal structures of **5d** (left) and **5d**•CO (right) with 35% thermal ellipsoids. Hydrogen atoms have been omitted for clarity. Selected bond lengths in **5d**: C(1)-Ni(1) = 1.746(12), C(2)-Ni(1) = 1.98(2), C(1)-O(1) = 1.081(12), C(2)-O(2) = 1.218(17), P(1)-Ni(1) = 2.172(3), P(2)-Ni(1) = 2.232(3) Å. Selected bond lengths in **5d**•CO: C(1)-Ni(1) = 1.867(4), C(2)-Ni(1) = 1.798(4), C(3)-Ni(1) =1.993(4), C(1)-O(1) = 1.133(4), C(2)-O(2) = 1.152(5), C(3)-O(3) = 1.211(4), P(1)-Ni(1) = 2.2094(10), P(2)-Ni(1) = 2.2802(10) Å.

Electron-Donating Ability of Ligands

The electron donating abilities of the bidentate phosphine ligands are evaluated by measuring the frequencies of the CO-stretching vibration of **4a** – **4f**. The ν_{CO} values are summarized in Table 1. For the series of ligands with the same Ar and Ar' substituents (Ar = *o*-methoxyphenyl and Ar' = 3,4-difluorophenyl) and different R (Figure 1), the electron donating ability follows the order **d** > **c** > **b**. The slightly stronger electron-donating ability of **d** than **c** is likely attributable to the lower steric hindrance of **d**, allowing more effective orbital overlaps between the P and Ni atoms. Comparison between **a**, **c**, and **f** confirms that the *o*-methoxy and *o*-methyl substituents increase the electron-donating ability of the ligand approximately to the same degree relative to a hydrogen atom. Between **e** and **b** that differ in the Ar' group on the borate center, **e** is somewhat more

Table 1. Comparison of the carbonyl stretching vibration ($\nu_{C\equiv O}$) of Ni(0) compounds.

compound	4a	4b	4c	4d	4e	4f
$\nu_{C\equiv O}$ (cm^{-1})	1988, 1927	1992, 1923	1979, 1915	1974, 1907	1985, 1921	1980, 1916

electron-donating as expected. Both **c** and **d** are more electron-donating than is **e**. Overall, the electron donating ability is ranked as **d** > **c** ≈ **f** > **e** > **a** > **b.**

Equilibriums of CO Insertion and Coordination

The equilibriums involving CO insertion and coordination (eq 1, Table 2) were studied in benzene and dichloromethane using ^{1}H NMR and IR spectroscopies. The qualitative observations are the same in benzene and dichloromethane. Under a nitrogen atmosphere, both a methyl peak and an acetyl peak are observable in ^{1}H NMR (at δ 0.5±0.1 and 1.8±0.3 ppm, respectively) in all cases in various amounts. Under 1 atm of CO, the methyl peak is present only for **d** but absent for the others according to ^{1}H NMR. The dynamic exchange between **5** and **6** is therefore slower than the detection time scale of ^{1}H NMR, and the equilibrium constant K_1 is very small (conservatively, $K_1 < 0.1$) for all except **d**. The 4-coordinate acetyl, **5**, is the most abundant species in all cases (eq 1) under 1 atm of CO, as assessed by the acetyl C=O stretching vibrations of **5** and **5**•CO at ~1690 and ~1710 cm^{-1}, respectively, in the IR spectra. For **c** and **e**, **5** is the only observable dominant species. For the others, **5**•CO co-exists with **5**. The equilibrium between **5**•CO and **5** is fast on the ^{1}H NMR time scale as only one dynamically averaged acetyl peak is observed. The equilibrium constant K_2 as well as K_1 for **d** in dichloromethane were determined from high-pressure IR and ^{1}H NMR data (see Experimental Section for details). The values of K_1 and K_2 are summarized in Table 2. The equilibrium constants in benzene were not quantified because **5**•CO has limited solubilities in benzene and precipitated at a low-concentration threshold when the CO pressure was raised.

Table 2. Equilibrium constants of zwitterionic Ni(II) compounds at 20 °C.

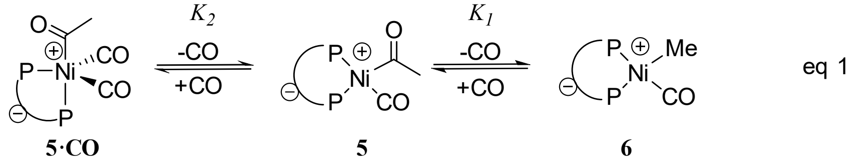

Suffix	a	b	c	d	e	f
K_1 (bar)	< 0.1[a]	< 0.1[a]	< 0.1[a]	0.14[b]	< 0.1[a]	< 0.1[a]
K_2 (bar)	7.2[b]	3.8[b]	150[b]	4.0[b]	21.5[b]	7.8[b]

[a] In both benzene and dichloromethane. [b] In dichloromethane.

In regard to the factors that affect the equilibrium constants, it appears a high degree of steric hindrance and a high electron-donating ability of the ligand favor the 4-coordinate over the 5-coordinate species (i.e., a large K_2) as exemplified by **c**. The electronic effect on K_2 is further corroborated by comparing **b** and **e**, which are sterically identical and only differ in their electron-donating ability. The reason is not clear why **d** has a more substantive K_1 value than the others.

Polymerization activity and productivity.

The performances of **5a – 5f** as catalysts for CO-ethylene copolymerization were evaluated. Toluene or THF were used as the polymerization medium at fixed CO and ethylene pressures (300 psi each), which we previously observed to be nearly optimal for the type of catalysts investigated here.[39] The polymerization was primarily studied at room temperature, but the effect of temperature was also examined in selective cases. Selective runs in 2, 5-dimethyltetrahydrofuran (DMTHF) were carried out to clarify the source of the solvent effect on the polymerization. A tabulated summary of all polymerization runs including the molecular weight of the products can be found in the Supporting Information (Table 1S).

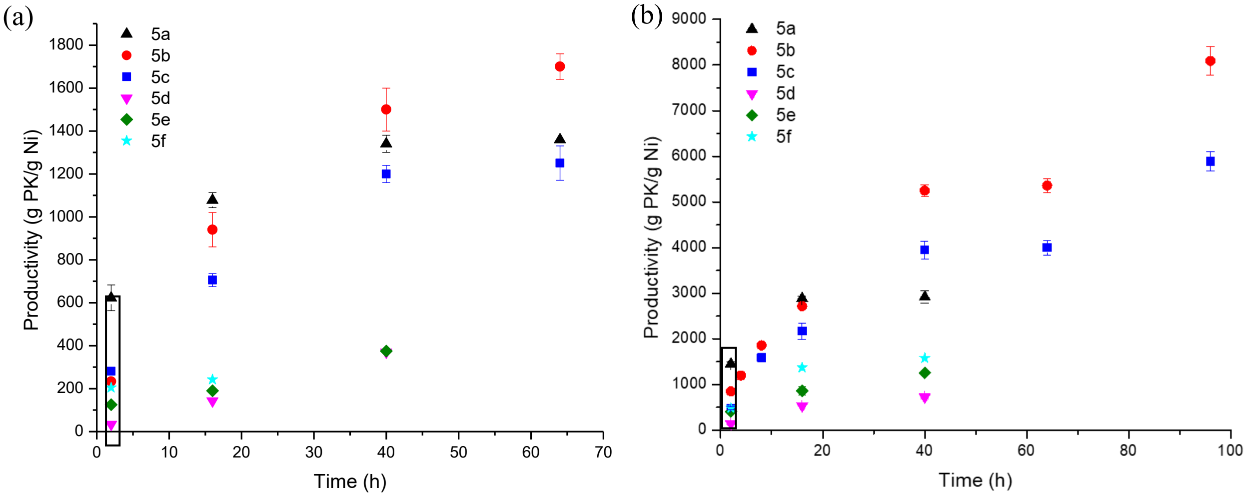

Figure 3. Productivity of catalysts **5a** – **5f** versus time in toluene (a) and THF (b) at room temperature under 300 psi each of CO and ethylene. The first set of data points enclosed in the boxes correspond to the polymerization time of 2 h.

The productivities of all catalysts as a function of time are plotted in Figure 3. Since the polymer product continuously precipitates, and the catalysts presumably continuously deactivate in the course of the reaction, the catalytic activity defined as the productivity per unit time is difficult to measure. We therefore use the productivity in the first 2 hours of polymerization (Figure 3) as an approximate indication of the inherent activity of the catalyst. Catalyst **5a** is considerably more active than the others in both toluene and THF. Comparison of **5a**, **5c** and **5f** shows that the *o*-methoxy substituent on the phenyl group of the phosphine ligands lowers the activity as does the methyl substituent. Among the catalysts that possess the *o*-methoxy substituent, further differences in the ligand steric and electronic properties give rise to differences in their activities to various extents. Most notable is the very low activity of **5d** in comparison to the others. This is likely attributable to its propensity of being trapped in the 5-coordinate dormant state (**5**•CO in eq 1). Comparison between **5b** and **5e**, the ligands of which have identical steric hindrance but differ in the electron-donating ability, suggest that a less electron-donating ligand results in a higher activity.

The *o*-methoxy substituent on the phenyl group of the ligand exerts a marked effect on the stability and ultimate productivity of the catalysts similar to what Drent previously disclosed for the cationic Ni catalysts.[9, 10] Catalyst **5a** deactivated between 16 and 40 h in both THF and toluene. In comparison, both **5b** and **5c** remain active after 40 h. The effect of the *o*-methoxy group is more dramatic in THF than in toluene. The apparent slow-down of the polymerization in THF (Figure 3(b)) catalyzed by **5b** and **5c** between 40 h and 64 h is caused by monomer depletion and the lack of mixing. For these runs when the autoclave was opened, the thick slurry of the solvent and polymer product stuck on the wall, and the area around the magnetic stirring bar at the bottom of the autoclave was dry. About 75-90% of the monomers are consumed assuming that they are ideal gases. When the polymerization was carried out in a larger autoclave with twice as much THF, a significant yield increase was observed from 64 to 96 h. We do not know for sure whether **5b** and **5c** were completely deactivated after 96 h, but these are the highest yields that the equipment in our laboratory allows to measure. The ability of the *o*-methoxy group to stabilize the catalyst cannot be attributed to a steric effect because **5f** deactivates much more quickly than **5b** and **5c** and in fact even more quickly than **5a** in both toluene and THF (Figure 3). Judging from the lack of interaction between Ni and the *o*-methoxy group in the ground state of the catalyst as revealed by their crystal structures and NMR spectra, we speculate that the *o*-methoxy group coordinates to Ni in an intermediate on the decomposition pathway and thus disrupts the decomposition.

The very long lifetime of **5b** and **5c** at room temperature prompted us to explore whether the high productivity could be obtained in a shorter period of reaction time at an elevated polymerization temperature. Unfortunately, when the polymerization was carried out at 45 °C, the yields after 16 h were only about 80% and 60% of those at room temperature for **5b** and **5c**, respectively (Figure 4). The thermal stabilities of both catalysts are limited under the polymerization conditions.

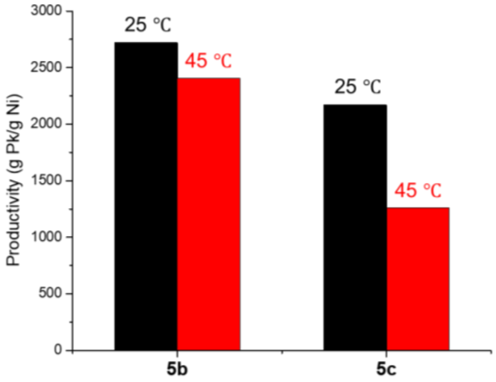

Figure 4. Productivity of **5b** and **5c** at different temperatures after polymerization for16 h.

All catalysts are 2-3 times more active in THF than they are in toluene. To answer the question whether the difference is caused by the polarity or coordination of THF, the polymerization was carried out in 2,5-dimethyltetrahydrofuran (DMTHF) using **5b** as a representative. The activity and productivity of **5b** in DMTHF are much lower than in THF and similar to those in toluene (Figure 5). Because DMTHF has a polarity similar to THF but a much-subdued coordination ability,[41] the results suggest that coordination of THF is largely responsible for the high activity and productivity of the polymerization in THF.

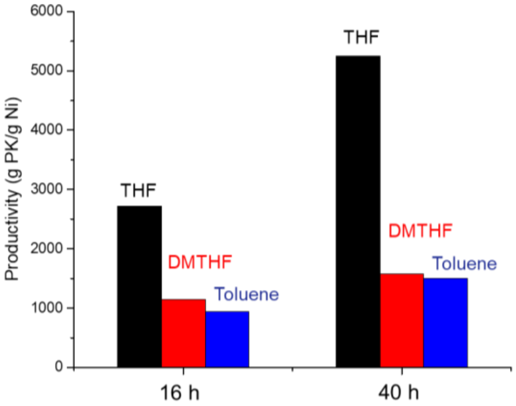

Figure 5. Productivity of **5b** in different solvents for polymerization runs for 16 and 40 h.

Polyketone Products

All catalysts produce the strictly alternating copolymers of CO and ethylene. A representative ^{1}H NMR of the product is shown in Figure 6. In addition to the ethylene ketone peak (d) at 2.85 ppm, a quartet and a triplet (b and a) are clearly observed at δ 2.58 and 1.08 ppm, respectively, attributable to an ethyl ketone group from sequential insertions of ethylene and CO into Ni-H afforded by β-hydrogen elimination. The vinyl ketone group from β-hydrogen elimination is observable at δ 6.74, 6.60, and 6.24 ppm (e, f, and c). The discrepancy in the concentrations of the vinyl ketone and the ethyl ketone will be discussed below. The peaks at δ 5.92 - 5.84 ppm are not assigned at the present time and will be discussed again below.

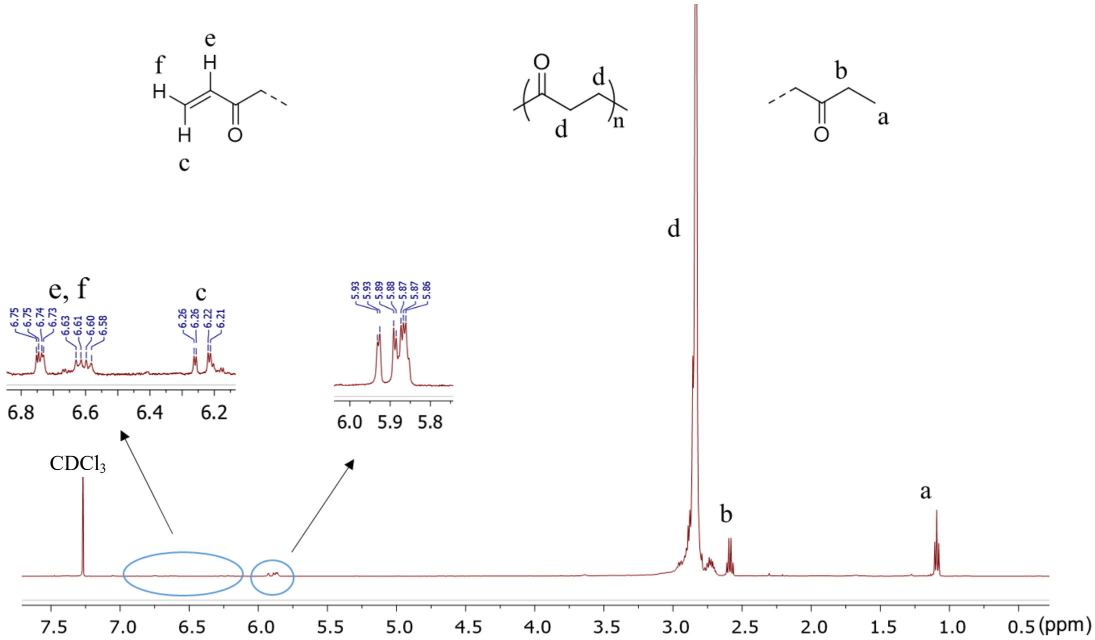

Figure 6. ^{1}H NMR spectrum with peak assignments of a representative polyketone product (entry 30, Table 1S in Supporting Information). The sample was dissolved in $CDCl_3$/TFA-d in a 10/1 volume ratio.

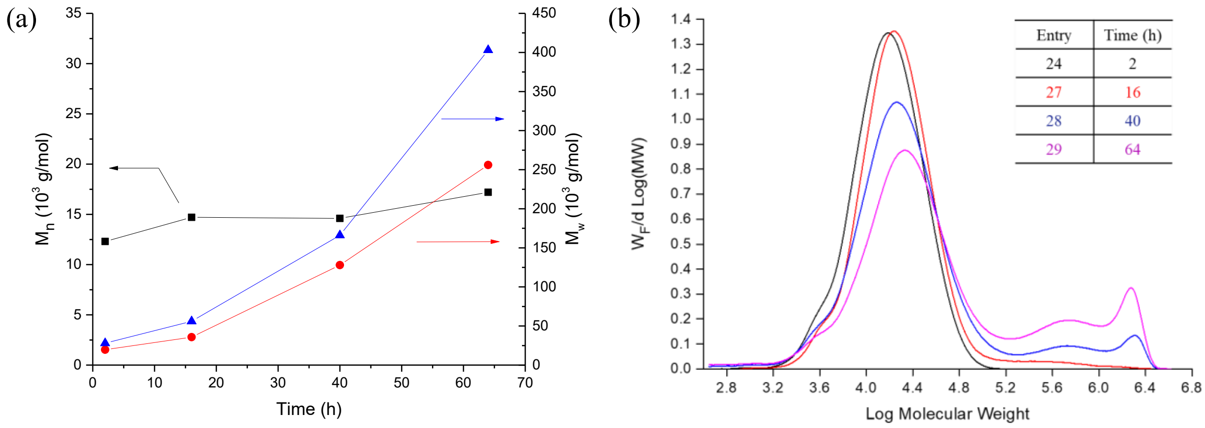

Figure 7. (a) M_n and M_w (▲ from static light scattering, ■ and ● from GPC relative to poly(methyl methacrylate) standards) as a function of polymerization time for polymerizations catalyzed by **5b**. (b) Molecular weight distribution of the same samples plotted as weight fraction vs log (molecular weight). The samples are from entries as indicated by the legend in Table 1S (see Supporting Information).

The weight-average molecular weight (M_w) of the products from runs of relatively high yields (i.e., polymerizations catalyzed by **5a** – **5c**) were determined by static light scattering using hexafluoroisopropyl alcohol (HFIPA) as the solvent, and further selective samples due to the high cost of the analysis were analyzed by gel permeation chromatography (GPC) by Smither Rappa to determine the number-average molecular weight (M_n) and M_w relative to poly(methyl methacrylate) standards using HFIPA as the eluent. There are no substantial differences in the molecular weights of the polyketones produced by **5a** – **5c** under the same polymerization conditions (see Table 1S in Supporting Information). The GPC and the light scattering results of the products from the polymerizations catalyzed by **5b** in THF are summarized in Figure 7 as representative examples. The M_n values of this series only increase slightly with the increase in polymerization time, but the M_w values increase considerably. The molecular weight distribution grows from approximately unimodal to bi-, tri-, or multi-modal with the polydispersity index increasing from 2 to 14 as the result. A similar trend in the molecular weights and molecular weight distributions is previously observed for polyketones produced by cationic Pd catalysts,[42] where a bimodal distribution of the molecular weight was fitted to a superimposed Flory-Schulz distribution for homogeneous catalysts and Wesslau distribution[43] for heterogeneous catalysts. The Flory-Schulz distribution was attributed to catalysts located in the external region of precipitated polymer particles, and the Wesslau distribution to catalytic sites located within the polymer matrix. A congested environment was suggested around the internalized catalytic sites, hampering the chain-transfer process. Consistent with such an assertion, the polymerizations catalyzed by **5b** in twice the amount of THF resulted in products with M_w = 26,000 g/mol (entry 30 in Table 1S in Supporting Information). Thus, internalization of the catalyst only happens when the polymer content in the reaction mixture is very high relative to the solvent content. Since the polymerizations in toluene do not reach such high yields as those in THF do due to the comparatively short catalyst lifetime in toluene, the very high molecular weight is not attained for polyketones produced in toluene.

Assuming that the ethyl ketone group is at the end of a linear polyketone chain, the M_n obtained by end group analysis is 3 – 4 times lower than the M_n obtained by GPC. Assuming that the vinyl ketone is the only end group at one end of the polymer chain, the M_n obtained by end group analysis is 4 – 7 times higher than the M_n obtained by GPC. A comparison of these data for the products obtained from the polymerizations catalyzed by **5b** in THF and toluene are shown in Figure 8 as an example of such discrepancies. To explain the discrepancies, we tentatively suggest that the

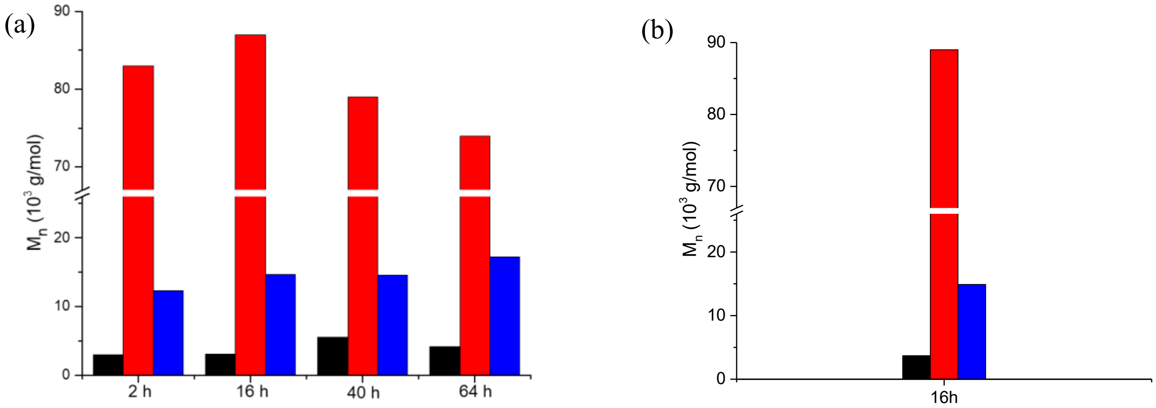

Figure 8. Discrepancies in M_n calculated by end group analysis using ethyl ketone (black) and vinyl ketone (red) and M_n from GPC (blue) for products of polymerizations catalyzed by **5b** in THF (a) and in Toluene (b).

examples of such discrepancies. To explain the discrepancies, we tentatively suggest that the polyketone product is branched as the result of re-insertion of the vinyl ketone group into a propagating chain at the Ni center. The peaks at δ 5.92 - 5.84 ppm account for the additional end groups and/or branching points, the identities of which we have not been able to recognize at the present time. Definitive characterization of the detailed structure of the product requires a comprehensive study involving synthesis of model organic compounds and GPC with a light scattering detector using HFIPA as the eluent. We do not have access to the GPC capability and leave such a study as a future possibility.

The thermal and mechanical properties of the alternating CO-ethylene copolymers are studied (see Supporting Information). The thermal decomposition with an onset at ~250 °C caused by residual Ni in the polyketone sample, as we previously reported,[39] remains observable even for the sample with the least Ni contamination (i.e., the polymerization run with the highest productivity in entry 30, Table 1S). The melting temperature of the polyketone is at 252 °C consistent with the reported values.[5,39] The polyketone is a brittle plastic with a Young modulus of 1.27 GPa, an engineering strength at break of 38.5 MPa, and a strain at break of 3.7%. The mechanical properties are unexceptional and consistent with the reported values.

SUMMARY

Zwitterionic Ni(II) complexes with various ancillary groups and borate anions on the bidentate anionic phosphine ligands are synthesized and studied as catalysts for the alternating copolymerization of CO and ethylene. A certain degree of steric crowding around the Ni(II) center is necessary to achieve a relatively high initial activity as evidenced by the very low activity of **5d** at least in part due to prevalence of the 5-coordinate dormant species under the polymerization conditions in the absence of sufficient steric hindrance. Too much steric hindrance reduces the activity as evidenced by the high activity of **5a** in comparison to **5b**, **5c** and **5f**. The ligand electronic effect on the catalytic activity is modest for the present range of catalysts. The copolymerization carried out in THF as the solvent is a few times faster than in toluene at room temperature for all catalysts. The solvent effect is attributed to the coordinated ability of THF rather than polarity. Detailed mechanisms of the effects of the coordinating solvent will be a focus of our future study. The *ortho*-methoxy substituent on the ligand phenyl ring markedly increases the catalyst life-time. Both **5b** and **5c**, which have the *ortho*-methoxy substituent, are markedly more productive overall than is **5a**, although **5a** displays a higher initial activity than **5b** and **5c** do. The effect of the *o*-methoxy group is of a coordinative origin rather than steric or inductive as the comparison between **5c** and **5f** suggests. All catalysts produce the alternating copolymer of CO and ethylene. The M_n values of all polyketone products are unexceptional on the order of 10^4 g/mol, while the M_w values and PDI increase with the polymerization time to the order of 10^5 g/mol. We tentatively suggest that the products are branched, but a detailed characterization of the structure requires future efforts.

EXPERMENTAL SECTION

All manipulations were performed in a nitrogen-filled glovebox or using standard Schlenk techniques. Solvents were purchased from Sigma-Aldrich and dried using an MBraun solvent purification system. All other chemicals were purchased from Sigma-Aldrich or VWR. Synthesis of **1g**, [38] **1h**, [39] **2j – 2l**, [39 40] **3a – 3c**, [39 40] **4a - 4c**,[39 40] **5b**,[40] and **5c**[40] were previously reported.

^{1}H,^{13}C,^{31}P, and ^{19}F NMR spectra were recorded on a Varian Mercury 300 MHz spectrometer or a Varian Avance 500 spectrometer. Chemical shifts were determined using solvent peaks as internal references for ^{1}H and ^{13}C NMR, the peak of 85% H_3PO_4 as an external reference for ^{31}P NMR, and the peak of hexafluorobenzene as an external reference for ^{19}F NMR. Elemental analyses were performed with an Elementar VARIO EL apparatus or by Micro Analysis, Inc. IR spectra in nujol mull were measured with an Excalibur Diglab instrument.High-pressure IR spectra were recorded with a ReactIR 702L instrument from Mettler Toledo with a silicon tipped probe.

GPC analysis was performed by Smithers Rapra & Smithers Pira Limited. Briefly, hexafluoroisopropyl alcohol was used as the eluent. A refractive index detector was used. The molecular weights of the polyketones were determined relative to poly(methyl methacrylate) standards.

Static light scattering analysis was performed on a Brookhaven Instruments light scattering spectrometer equipped with a diode-pumped solid-state (DPSS) laser operating at 633 nm and a BI-9000AT multichannel digital correlator. The M_w was obtained by Zimm plot using Brookhaven light scattering software. Zimm plots of all measurements are provided in the Supporting Information.

Synthesis of 1i. In a nitrogen filled glovebox, a 25-ml flask containing a magnetic stirring bar was charged with $Pd(OAc)_2$ (56 mg, 2.5 mmol), 2,4-dibromoiodobenzne (3.6 g, 10 mmol), Et_3N (10 mL), and di-*o*-tolylphosphine (2.14 g, 10 mmol). The flask was removed from the glovebox, and the mixture was heated to reflux and magnetically stirred for 3 days. The solvent was removed. The solid residue was dissolved in toluene and filtered. The crude product was recrystallized in ethanol. Yield, 3.4g (75%). ^{1}H NMR (300 MHz, $CDCl_3$): δ (ppm) 7.79 (s, 1H), 7.38 – 7.24 (m, 5H), 7.11 (s, 2H), 6.72 (m, 2H), 6.59 (d, *J* = 8.2 Hz, 1H), 2.41 (s, 6H). ^{31}P{^{1}H} NMR (121 MHz, $CDCl_3$): δ (ppm) -20.4. ^{13}C{^{1}H} NMR (126 MHz, $CDCl_3$): δ (ppm) 142.9 (s, *i*-P($C_6H_5CH_3$)), 142.7 (s, *i*-$CH_3C_6H_5$), 137.2 (d, *o*-P($C_6H_3Br_2$)), 135.5 (dd, *i*-P($C_6H_3Br_2$)), 133.4 (d, *m*-P($C_6H_3Br_2$)), 133.1 (s, *o*-P($C_6H_5CH_3$)), 130.9 (d, *m*-P($C_6H_3Br_2$)), 130.8 (s, *m*-P($C_6H_5CH_3$)), 130.3 (d, *o*-P($C_6H_5CH_3$)), 129.2 (s, *p*-P($C_6H_5CH_3$)), 126.4 (s, *m*-P($C_6H_5CH_3$)), 123.4 (s, *p*-P($C_6H_3Br_2$)), 21.1 (d, *o*-$C_6H_4CH_3$).

Synthesis of 2m. Compound **1h** (1.40 g, 2.90 mmol) was dissolved in 170 mL Et_2O. The solution was cooled to -78 °C. ^{n}BuLi (1.90 mL, 1.6 M in cyclohexane) was injected into the above solution. The mixture was stirred and turned a white suspension in 5 min. After 4 h at -78 °C, $ClPEt_2$ (0.365 g, 2.92 mmol) was added. The cold bath was removed, and the reaction was stirred for 8 h. The solvent was removed. $CHCl_3$ was used to extract the product. The solution was filtered. $CHCl_3$ was removed. The product was crystallized in hot EtOH. Yields, 0.76 g (53%). ^{1}H NMR (300 MHz, $CDCl_3$): δ (ppm) 7.56 – 7.53 (m, 1H, Ar*H*), 7,34 – 7.26 (m, 3H, Ar*H*), 6.88 – 6.81(m, 4H, Ar*H*), 6.76 – 6.72 (m, 1H, Ar*H*), 6.65 (b, 2H, Ar*H*), 3.71 (s, 6H, ArOCH_3), 1.72 – 1.62(m, *J* = 30 Hz, 4H, P(CH_2CH_3)$_2$), 1.00 – 0.90 (m, *J* = 30 Hz, 6H, P(CH_2CH_3)$_2$). ^{31}P{^{1}H} NMR (121 MHz, $CDCl_3$): δ (ppm) -25.3(d, J = 164.6 Hz), -35.5(d, J = 164.6 Hz). ^{13}C{^{1}H} NMR (75 MHz, $CDCl_3$): δ (ppm) 161.2 (d, *J* = 15.9 Hz, *m*-P($C_6H_4OCH_3$)), 147.3 (dd, *J* = 20.3, 12.8 Hz, *m*-Br($C_6H_3P_2$)), 143.1 (dd, *J* = 30.4, 10.5 Hz, *p*-Br($C_6H_3P_2$)), 135.5 (d, *J* = 6.4 Hz, *m*-Br($C_6H_3P_2$)), 134.2 (s, *o*-P($C_6H_4OCH_3$)), 132.4 (dd, *J* = 7.2, 2.1 Hz, *o*-Br($C_6H_3P_2$)), 131.6 (s, *p*-P($C_6H_4OCH_3$)), 130.1 (s, *i*-P($C_6H_4OCH_3$)), 125.2 (dd, *J* = 14.8, 5.7 Hz, *o*-Br($C_6H_3P_2$)), 123.9 (d, *J* = 2.0 Hz, *i*-Br($C_6H_3P_2$)), 120.9 (s, *m*-P($C_6H_4OCH_3$)), 110.2 (d, *J* = 1.5 Hz), 77.4 ($CDCl_3$), 55.7 (d, *J* = 1.1 Hz, P($C_6H_4OCH_3$)$_2$), 20.1 (s, P(CH_2CH_3)$_2$), 9.8 (d, *J* = 13.0 Hz, P(CH_2CH_3)$_2$). Anal. Calcd for $C_{24}H_{27}O_2P_2Br$: C, 58.91; H, 5.56; Found: C, 59.15; H, 5.72.

Synthesis of compound 2n. This was prepared in a manner analogous to that for **2m**, except that **1i** (2 mmol) and ClP^{i}Pr$_2$ (2 mmol) were used, in 62% yield. ^{1}H NMR (300 MHz, $CDCl_3$): δ (ppm) 7.63 (dd, *J* = 3.5, 1.8 Hz, 1H, Ar*H*), 7.37 – 7.32 (m, 1H, Ar*H*), 7.32 – 7.16 (m, 5H, Ar*H*), 7.06 (m, 2H, Ar*H*), 6.73 (m, 2H, Ar*H*), 2.55 – 2.36 (m, 6H, *o*-PhCH_3), 2.13 – 1.97 (m, 2H,

$\mathrm{PC}H(\mathrm{CH_3})_2$), 1.11 (dd, *J* = 14.4, 7.0 Hz, 6H, $\mathrm{PCH(C}H_3)_2$), 0.82 (m, 6H, $\mathrm{PCH(C}H_3)_2$). $^{31}\mathrm{P}\{^{1}\mathrm{H}\}$ NMR (121 MHz, $\mathrm{CDCl_3}$): δ (ppm) -1.7 (d, *J* = 155.4 Hz), -27.9 (d, *J* = 155.1 Hz). $^{13}\mathrm{C}\{^{1}\mathrm{H}\}$ NMR (126 MHz, $\mathrm{CDCl_3}$): δ (ppm)145.5 (dd, *J* = 31.7, 23.2 Hz, *m*-Br($C_6\mathrm{H_3P_2}$)), 144.7 (dd, *J* = 32.4, 10.5 Hz, *p*-Br($C_6\mathrm{H_3P_2}$)), 142.5 (s, *i*-P($C_6\mathrm{H_5CH_3}$)), 142.3 (s, *o*-P($C_6\mathrm{H_5CH_3}$)), 135.7 (s, *m*-Br($C_6\mathrm{H_3P_2}$)), 135.7 – 134.6 (m, *o*-Br($C_6\mathrm{H_3P_2}$)), 134.1 (s, *o*-Br($C_6\mathrm{H_3P_2}$)), 131.07 (s, *o*-P($C_6\mathrm{H_5CH_3}$)), 129.9 (d, *J* = 4.8 Hz, *m*-P($C_6\mathrm{H_5CH_3}$)), 128.4 (s, *p*-P($C_6\mathrm{H_5CH_3}$)), 125.8 (s, *m*-P($C_6\mathrm{H_5CH_3}$)), 123.2 (d, *J* = 2.3 Hz, *i*-Br($C_6\mathrm{H_3P_2}$)), 24.8 (m, $\mathrm{P}C\mathrm{H(CH_3)_2}$), 21.4 (d, *J* = 21.4 Hz, *o*-$\mathrm{C_6H_5}C\mathrm{H_3}$), 20.0 (d, *J* = 18.4 Hz, $\mathrm{PCH(}C\mathrm{H_3)_2}$), 19.3 (d, *J* = 10.7 Hz, $\mathrm{PCH(}C\mathrm{H_3)_2}$).

Synthesis of 3d. Compound **2m** (0.70 g, 1.35 mmol) was dissolved in 50 mL THF. The solution was cooled to -78 °C. ^{n}BuLi (0.86 mL, 1.6 M in cyclohexane, 1.39 mmol) was injected into the above solution via a syringe. The solution was stirred for 1 h. Then, solid tris(3,4-difluorophenyl)borane (0.475 g, 1.36 mmol) was added to the above solution. The reaction was warmed to room temperature in 1 h. The solvent was removed to give a foamy solid. The solid was dissolved in dimethoxyethane (DME) (10 mL), and then DME was removed under vacuum. The product was dissolved in $\mathrm{CHCl_3}$, and hexane was layered over the solution. A crystalline compound was obtained at room temperature. Yield, 1.01 g (83%). ^{1}H NMR (500 MHz ,$\mathrm{CD_3CN}$): δ (ppm) 7.44 (b, 2H, Ar*H*), 7.35 – 7.30 (m, 2H, Ar*H*), 7.03 – 6.93(m, 11H, Ar*H*), 6.87 – 6.82(m, 2H, Ar*H*), 6.63(b, 2H, Ar*H*), 6.52(b, 1H, Ar*H*), 3.70(s, 6H, $\mathrm{ArO}CH_3$), 3.46(s, 2H, $\mathrm{CH_3O}CH_2$), 3.52(s, 3H, $CH_3\mathrm{OCH_2}$), 1.98(m, $\mathrm{CD_3CN}$), 1.57 – 1.48(m, *J* = 27 Hz, 4H, $\mathrm{P(}CH_2\mathrm{CH_3)_2}$), 0.90 – 0.81(m, *J* = 27 Hz, 6H, $\mathrm{P(CH_2}CH_3\mathrm{)_2}$). $^{31}\mathrm{P}\{^{1}\mathrm{H}\}$ NMR (203 MHz, $\mathrm{CD_3CN}$): δ (ppm) -26.1 (d, *J* = 160.9Hz), -36.5 (d, *J* = 160.9Hz). ^{19}F NMR (470 MHz, $\mathrm{CD_3CN}$): δ (ppm) -145.1 (m), -149.9 (m). $^{13}\mathrm{C}\{^{1}\mathrm{H}\}$NMR (126 MHz, $\mathrm{CD_3CN}$): δ 162.4 (q, *J* = 50.4 Hz, *i*-B($C_6\mathrm{H_3F_2}$)), 161.0 (d, *J* = 16.4 Hz, *m*-P($C_6\mathrm{H_4OCH_3}$)), 159.8 (ddd, *J* = 99.1, 49.5, 4.3 Hz, *m*-B($C_6\mathrm{H_3F_2}$)), 149.1 (dddd, *J* = 242.8, 11.5, 8.0, 3.8 Hz, *p*-B($C_6\mathrm{H_3F_2}$)), 146.8 (dd, *J* = 238.9, 13.0 Hz, *m*-B($C_6\mathrm{H_3F_2}$)), 140.0 (m, *m*-B($C_6\mathrm{H_3P_2}$)), 137.5 (d, *J* = 7.2 Hz, *p*-B($\mathrm{C_6H_3P_2}$)), 135.8 (s, *m*-B($C_6\mathrm{H_3P_2}$)), 135.7 (dd, *J* = 31.2, 6.4 Hz, *o*-B($C_6\mathrm{H_3P_2}$)), 134.0 (s, *o*-P($C_6\mathrm{H_4OCH_3}$)), 131.7 (s, *o*-B($C_6\mathrm{H_3P_2}$)), 130.9 (dt, *J* = 5.0, 2.7 Hz, *p*-P($C_6\mathrm{H_4OCH_3}$)), 129.6 (s, *i*-P($C_6\mathrm{H_4OCH_3}$)), 127.2 (dd, *J* = 17.6, 5.2 Hz, *o*-B($C_6\mathrm{H_3F_2}$)), 122.5 (dd, *J* = 12.4, 2.6 Hz, *o*-B($C_6\mathrm{H_3F_2}$)), 120.7 (s, *m*-P($C_6\mathrm{H_4OCH_3}$)), 117.3 (s, $\mathrm{CD_3CN}$), 114.3 (ddd, *J* = 14.6, 6.6, 3.0 Hz, *i*-B($\mathrm{C_6H_3P_2}$)), 110.5 (d, *J* = 1.5 Hz, *m*-P(*C*6$\mathrm{H_4OCH_3}$)), 71.2 (d, *J* = 2.0 Hz, $C\mathrm{H_2OCH_3}$), 58.0 (s, $\mathrm{CH_2O}C\mathrm{H_3}$), 55.2 (s, $\mathrm{P(C_6H_4O}C\mathrm{H_3)}$), 19.4 (s, $\mathrm{P(}C\mathrm{H_2CH_3)}$), 9.2 (d, *J* = 13.2 Hz, $\mathrm{P(CH_2}C\mathrm{H_3)}$), 0.4 (dq, *J* = 41.5, 20.9 Hz, $\mathrm{CD_3CN}$). HRMS (MALDI): m/z calcd for $\mathrm{C_{42}H_{36}O_2BF_6P_2}$:759.2193 [M−Li(DME)$_n^+$], found 759.3069.

Synthesis of 4d. $\mathrm{Ni(COD)_2}$ (0.30 g, 1.09 mmol) was loaded into a 100-mL 3-neck flask and dispersed in DME (10 mL). Ligand **3d** (0.85 g, 1.0 mmol) was dissolved in DME (15 ml) and charged into an additional funnel. The addition funnel was attached to the flask under nitrogen. The nitrogen atmosphere was replaced with an CO atmosphere (1 atm). The suspension in the flask was stirred. When $\mathrm{Ni(COD)_2}$ was completely converted to $\mathrm{N(CO)_4}$ as indicated by the cease of CO uptake, the **3d** solution in the additional funnel was added into the flask. The solution was stirred for 4 h under CO. All volatile components were removed under vacuum into a liquid nitrogen-cooled trap. The cold trap was exposed to air to decompose any $\mathrm{Ni(CO)_4}$ in the trap. The foamy solid in the flask was extracted with DME (15 mL). After filtration, the volume of the solution was reduced to ~5 mL, and hexane (10 mL) was layered on top of the remaining solution. A light-yellow crystalline compound was obtained. Yield, 0.76 g (84%). ^{1}H NMR (300 MHz, $\mathrm{CD_2Cl_2}$) δ (ppm): 7.66 (s, 1H, Ar*H*), 7.38 – 7.25 (m, 2H, Ar*H*), 7.22 (s, 1H, Ar*H*), 7.03 – 6.78 (m, 16H, Ar*H*), 3.65 (s, 6H, ArOCH3), 3.64 (s, 8H, $\mathrm{C}H_2\mathrm{OCH_3}$), 3.45 (s, 12H, $\mathrm{CH_2OC}H_3$), 1.81 – 1.66 (m, 4H, $\mathrm{P(C}H_2\mathrm{CH_3)_2}$), 0.90 – 0.73 (m, 6H, $\mathrm{P(CH_2C}H_3\mathrm{)_2}$). $^{31}\mathrm{P}\{^{1}\mathrm{H}\}$ NMR (121 MHz, $\mathrm{CD_2Cl_2}$) δ (ppm): 43.5

(d, *J* = 31.46 Hz), 27.6 (d, *J* = 31.46 Hz). ^{19}F NMR (282 MHz, CD_2Cl_2) δ (ppm): -144.6 (m), -149.4 (m). ^{13}C{^{1}H} NMR (126 MHz, CD_2Cl_2): δ (ppm) 202.5 (s, Ni($CO)_2$), 163.8 (dd, *J* = 100.1, 48.7 Hz, *i*-B($C_6H_3F_2$)), 160.5 (d, *J* = 8.2 Hz, *m*-P($C_6H_4OCH_3$)), 159.3 (dd, *J* = 99.8, 49.5 Hz, *m*-B($C_6H_3F_2$)), 149.2 (d, *J* = 243.0 Hz, *p*-B($C_6H_3F_2$)), 146.9 (dd, *J* = 239.6, 13.2 Hz, *m*-B($C_6H_3F_2$)), 140.5 (d, *J* = 39.2 Hz, *m*-B($C_6H_3P_2$)), 138.6 (m, *p*-B($C_6H_3P_2$)), 137.1 (s, *m*-B($C_6H_3P_2$)), 136.8 (d, *J* = 13.0 Hz, *o*-B($C_6H_3P_2$)), 132.5 (d, *J* = 4.4 Hz, *o*-P($C_6H_4OCH_3$)), 130.8 (d, *J* = 3.9 Hz, *o*-B($C_6H_3P_2$)), 130.66(*p*-P($C_6H_4OCH_3$)), 130.1 (s, *i*-P($C_6H_4OCH_3$)), 125.9 (d, *J* = 31.5 Hz, *o*-B($C_6H_3F_2$)), 122.7 (d, *J* = 11.9 Hz, *o*-B($C_6H_3F_2$)), 120.1 (d, *J* = 6.1 Hz, *m*-P($C_6H_4OCH_3$)), 114.1 (d, *J* = 13.0 Hz, *i*-B($C_6H_3P_2$)), 110.8 (s, *m*-P($C_6H_4OCH_3$)), 70.5 (s, CH_2OCH_3), 59.4 (s, CH_2OCH_3), 55.2 (s, P($C_6H_4OCH_3$)), 53.4 (dt, *J* = 54.5, 27.2 Hz, CD_2Cl_2), 23.7 (dd, *J* = 18.1, 6.4 Hz, P(CH_2CH_3)), 8.4 (d, *J* = 5.2 Hz, P(CH_2CH_3)). HRMS (MALDI): m/z calcd for $C_{44}H_{36}O_4BF_6P_2Ni$: 873.1337[M−Li(DME)$_n^+$], found 873.2212.

Synthesis of 4e. Diphosphine **2l** (0.89 g, 1.60 mmol) was dissolved in THF (50 mL) and cooled to -78°C. n-BuLi (1.0 ml, 1.60 M in hexane, 1.60 mmol) was injected into the solution. The solution was stirred for 2 hours. Then tri(*o*-tolyl) borane (0.448 g, 1.60 mmol) was added as a solid. Solution was stirred for another 2 hours. The solvent was removed to get the crude product, **3e**. The crude **3e** was used for next step without purification. Ni(COD)$_2$ (0.420 g, 1.53 mmol) and DME (15 mL) were added into the flask. The flask was charged with carbon monoxide. The solution was stirred for 2 hours. Then solvent was removed. The crude product was crystallized upon diffusion of hexane (10 mL) layered on top of its DME solution (10 mL). Yield 0.85 g (60%). ^{1}H NMR (500 MHz, CD_2Cl_2): δ (ppm) 7.51 (s, 1H, Ar*H*), 7.24 (m,16H, Ar*H*), 6.95 – 6.74 (m, 18H, Ar*H*), 3.61 (s, 6H, ArOCH_3), 3.58 (s, 12H, CH_2OCH_3), 3.41 (s, 18H, CH_2OCH_3) 1.54(s, 9H, BArCH_3). ^{31}P{^{1}H} NMR (202 MHz, CD_2Cl_2): δ (ppm) 45.8, 27.2. ^{13}C{^{1}H} NMR (126 MHz, CD_2Cl_2): δ (ppm) 201.4 (s, Ni($CO)_2$), 161.3 (m, *i*-B($C_6H_4CH_3$)), 160.6 (m, *m*-P($C_6H_4OCH_3$)), 143.4 (s, *m* or *p*-B($C_6H_3P_2$)), 139.5 (m, *o*-B($C_6H_4CH_3$)),136.0 (m, *i*-P(C_6H_5)), 132.2 (m, *o*-P($C_6H_4OCH_3$), *o*-B($C_6H_4CH_3$), *o*-P(C_6H_5) and *m*-B($C_6H_3P_2$)), 129.9 (s, *o*-B($C_6H_3P_2$)), 129.1 (m, *p*-P($C_6H_4OCH_3$)),122.8 (s, *m*-B($C_6H_4CH_3$)), 127.7 (m, *m* or *p*-P(C_6H_5)),122.9 (s, *i*-P($C_6H_4OCH_3$)), 122.56 (s, *m*-B($C_6H_4CH_3$)), 120.0 (d, *J* = 6.2 Hz, *m*-P($C_6H_4OCH_3$)), 110.6 (s, *m*-P($C_6H_4OCH_3$)), 70.9 (s, CH_2OCH_3), 59.2 (s, CH_2OCH_3), 55.1 (s, P($C_6H_4OCH_3$)), 53.4 (m, CD_2Cl_2), 24.4 (s, B($C_6H_4CH_3)_3$). HRMS (MALDI): m/z calcd for $C_{55}H_{48}O_4BP_2Ni$: 903.2480 [M-Li(DME)$_3^+$], found 903.2628.

Synthesis of 4f. This was prepared in a manner analogous to that for **4e** with the yield of 80%. ^{1}H NMR (300 MHz, CD_2Cl_2): δ (ppm) 7.58 (s, 1H, Ar*H*), 7.22 – 7.16 (m,4H, Ar*H*), 7.04 – 6.77 (m, 14H, Ar*H*), 6.72 (m, 1H, Ar*H*), 3.51 (s, 9H, DME(OCH_2CH_3)), 3.33 (s, 14H, DME(OCH_2CH_3)), 2.66 (s, 3H, *o*-PhCH_3), 2.31 (m, 2H, P$CH(CH_3)_2$), 2.06 (s, 3H, *o*-PhCH_3), 1.19 (m, 6H, P$CH(CH_3)_2$), 0.71 (m, 6H, P$CH(CH_3)_2$). ^{31}P{^{1}H} NMR (121 MHz, CD_2Cl_2): δ (ppm) 70.08 (d, *J* = 32.2 Hz), 31.42 (d, *J* = 32.4 Hz). ^{19}F NMR (282 MHz, CD_2Cl_2): δ (ppm) -144.6 (m), -149.3 (m). ^{13}C{^{1}H} NMR (126 MHz, CD_2Cl_2): δ (ppm) 204.4 (s, Ni(CO)), 200.7 (s, Ni(CO)), 164.2 (dd, *J* = 99.1, 49.9 Hz, *i*-B($C_6H_3P_2$)), 159.2 (dd, *J* = 101.4, 51.7 Hz, *i*-B($C_6H_3F_2$)), 149.3 (d, *J* = 243.1 Hz, *m*-B($C_6H_3F_2$)), 147.0 (dd, J = 239.6, 13.2 Hz, *p*-B($C_6H_3F_2$)), 141.6 (m, *m* or *p*-B($C_6H_3P_2$)), 139.2 (d, *J* = 12.3 Hz, *m* or *p*-B($C_6H_3P_2$)), 137.6 (d, J = 43.0 Hz, *o*-B($C_6H_3P_2$)), 137.2 (s, *o*-B($C_6H_3P_2$)), 134.8 (s, *m*-B($C_6H_3P_2$)), 131.4 (d, J = 27.7 Hz, *i*-P($C_6H_4CH_3$)), 132.1 (s, *m*-P($C_6H_4CH_3$)), 130.9 (s, *p*-P($C_6H_4CH_3$)), 128.5 (d, *J* = 45.4 Hz, *o*-P($C_6H_4CH_3$)), 125.0 (d, *J* = 5.6 Hz, *o*-P($C_6H_4CH_3$)), 122.7 (d, *J* = 12.3 Hz, *o*-B($C_6H_3F_2$)), 120.7 (dd, *J* = 77.0, 12.5 Hz, *m*-B($C_6H_3F_2$)), 115.1 (m, *p*-P($C_6H_4CH_3$)), 114.1 (ddd, J = 14.3, 6.7, 3.2 Hz, *o*-B($C_6H_3F_2$)), 27.9 (m, P$CH(CH_3)_2$), 25.4 (m, P$CH(CH_3)_2$), 22.4 (d, *J* = 12.0 Hz, P(*o*-$C_6H_4CH_3$)), 21.4 (d, *J* = 12.7 Hz, P(*o*-$C_6H_4\mathit{C}H_3$)), 19.6 (d, *J* = 8.5 Hz, $PCH(\mathit{C}H_3)_2$), 19.03 (d, *J* = 11.1 Hz, $PCH(\mathit{C}H_3)_2$), 18.6 (s, $PCH(\mathit{C}H_3)_2$), 17.7 (s, $PCH(\mathit{C}H_3)_2$). HRMS (MALDI): m/z calcd for $C_{46}H_{40}O_2BF_6P_2Ni$: 869.1860 [M-Li(DME)$_3^+$], found 869.1896.

Synthesis of 5a. In a 25-mL Schlenk flask with **4a** (500 mg, 0.45 mmol) and $Me_3O^+BF_4^-$ (200 mg, 1.35mmol) were charged CH_2Cl_2 (10 mL) at -30 °C. The suspension was put under CO (1 atm) and stirred for 6 h at -30 °C. Then, hexane (30 mL) was added to precipitate the solid mixture. After the solution was filtered, toluene (30 mL x 3) was used to extract the solid. The solution was filtered to remove the solid. The volume of the solution was reduced to ~20 mL under vacuum. Hexane (40 mL) was layered on top of the solution. The flask was kept at -45 °C. The precipitated yellow power was washed with diethyl ether (3 mL). Yield, 220 mg (56%). ^1H NMR (300 MHz, Benzene-*d*$_6$): δ (ppm) 7.97 – 7.79 (m, 3H, Ar*H*), 7.39 (m, 4H, Ar*H*), 7.12 (m, 3H, Ar*H*), 7.05 – 6.86 (m, H, Ar*H*), 6.83 (dt, *J* = 6.7, 3.7 Hz, 4H, Ar*H*), 1.82 – 1.61 (m, 2H, $PC\mathit{H}(CH_3)_2$), 1.52 (s, 3H, $NiCOC\mathit{H}_3$), 0.54 (ddd, *J* = 39.9, 17.0, 7.0 Hz, 12H, $PCH(C\mathit{H}_3)_2$). $^{31}P\{^1H\}$ NMR (121 MHz, C_6D_6): δ (ppm) 73.2, 40.3. ^{19}F NMR (282 MHz, C_6D_6): δ (ppm) -142.7 (m), -146.9 (m). Anal. Calc for $C_{45}H_{39}BOF_6P_2Ni$, C: 64.25, H: 4.67; Found: C: 64.51, H: 4.76.

Synthesis of 5d. Compound **4d** (500 mg, 0.43 mmol) and $Me_3O^+BF_4^-$ (192 mg, 1.3 mmol) were both dissolved in 10ml CH_2Cl_2. Solution was stirred under CO for 6 hours at -30 °C. After reaction, 30ml hexane was added to precipitate the product. Then the solution was filtered. Toluene (20*3 mL) was used to extract the solid. Toluene was then reduced to ~20 mL under vacuum and layered with hexane (40 mL). The flask was placed under -45°C. Yield, 278 mg (71%). ^1H NMR (300 MHz, CD_2Cl_2): δ (ppm) 7.74 (s, 1H), 7.67 – 7.50 (m, 3H), 7.15 (td, *J* = 8.0, 2.3 Hz, 2H), 7.09 – 7.02 (m, 3H), 7.01 – 6.82 (m, 10H), 3.77 (s, 6H, $ArOC\mathit{H}_3$), 2.10 – 1.85 (m, 4H, $P(\mathit{CH}_2CH_3)_2$), 0.81 (dt, *J* = 19.3, 7.6 Hz, 6H, $P(CH_2\mathit{CH}_3)_2$), 0.65 (dd, *J* = 7.6, 3.1 Hz, 3H, $Ni\mathit{CH}_3$). $^{31}P\{^1H\}$ NMR (121 MHz, CD_2Cl_2): δ (ppm) 60.54(d, *J* = 33.9Hz), 36.53(d, *J* = 33.9Hz). ^{19}F NMR (282 MHz, CD_2Cl_2): δ (ppm) -143.8 (m), -148.5 (m). $^{13}C\{^1H\}$ NMR (126 MHz, CD_2Cl_2): δ (ppm) 211.5 (s, Ni(*C*O)),170.3 (m, *i*-B($C_6H_3F_2$)), 159.9 (d, *J* = 7.5 Hz, *m*-P($\mathit{C}_6H_4OCH_3$)), 158.5 (m, *m*-B($\mathit{C}_6H_3F_2$)), 149.3 (d, *J* = 245Hz, *p*-B($\mathit{C}_6H_3F_2$)), 147.4 (d, *J* = 241 Hz, *m*-B($C_6H_3F_2$)), 140.6 (s, *m*-B($\mathit{C}_6H_3P_2$)), 138.6 (d, *J* = 16.1 Hz, *p*-B($\mathit{C}_6H_3P_2$)), 133.7 (s, *m*-B($\mathit{C}_6H_3P_2$)), 133.2 (d, *J* = 2.6 Hz, *o*-B($\mathit{C}_6H_3P_2$)), 130.6 (s, *o*-P($\mathit{C}_6H_4OCH_3$)), 128.5 (d, *J* = 102.0 Hz, *o*-B($\mathit{C}_6H_3P_2$)), 128.2 (s, *p*-P($\mathit{C}_6H_4OCH_3$)), 125.2 (s, *i*-P($\mathit{C}_6H_4OCH_3$)), 122.6 (d, *J* = 15 Hz, *o*-B($C_6H_3F_2$)), 122.58(d, *J* = 7.5 Hz, *o*-B($\mathit{C}_6H_3F_2$))116.08 (d, *J* = 50.2 Hz, *m*-P($\mathit{C}_6H_4OCH_3$)), 114.5 (m, *i*-B($\mathit{C}_6H_3P_2$)), 111.5 (d, *J* = 5.1 Hz, *m*-P($\mathit{C}_6H_4OCH_3$)), 55.34 (s, P($C_6H_4O\mathit{C}H_3$)), 19.2 (d, *J* = 32.4 Hz, P($\mathit{C}H_2CH_3$)), 8.4 (s, P($CH_2\mathit{C}H_3$)), -3.39 (d, *J* = 22.1 Hz, Ni($\mathit{C}H_3$)). Anal. Calc for $C_{44}H_{36}O_4BF_6P_2Ni$, C: 60.45, H: 4.15; Found: C: 60.83, H: 4.57.

Synthesis of 5e. Compound **4e** (500 mg, 0.423 mmol) and $Me_3O^+BF_4^-$ (200 mg, 1.35 mmol) were dissolved in CH_2Cl_2(8 mL). The mixture was stirred under CO at -30°C for 6 h. After 6 h, hexane (30 mL) was added to the orange solution. The mixture was stirred to give copious precipitate. The solvent mixture of hexane and CH_2Cl_2 was removed by filtration. A large amount of toluene (100 x 3 mL) was used to extract the product. The solution was concentrated to ~20 mL. Hexane (50 mL) was layered on top of the toluene solution. The mixture was kept at -45°C to allow diffusion. Yield, 221 mg (58%). ^1H NMR (300 MHz, CD_2Cl_2): δ (ppm) 7.61 (s, 1H, Ar*H*), 7.57 – 7.39 (m, 6H, Ar*H*), 7.32 (s, 3H, Ar*H*), 7.29 – 7.12 (m, 8H, Ar*H*), 7.03 (d, 4H, ArH), 6.95 – 6.78 (m, 13H, Ar*H*), 3.83 (s, 6H, $ArOC\mathit{H}_3$), 2.00 (s, 3H, $NiCOC\mathit{H}_3$), 1.54(s, 9H, $BArC\mathit{H}_3$). $^{31}P\{^1H\}$ NMR (121 MHz, CD_2Cl_2): δ (ppm) 40.2, 23.7. Anal. Calc for $C_{55}H_{51}O_3BP_2Ni$, C: 74.10, H: 5.77; Found: C: 74.72, H: 5.77.

Synthesis of 5f. This was prepared in a manner analogous to that for **5d**, except that **4f** was used as the starting material, in 70% yield. ^{1}H NMR (300 MHz, C_6D_6): δ (ppm) 7.95 -7.84 (d, 1H, Ar*H*), 7.44 (d, 3H, Ar*H*), 7.18 (d, *J* = 9.1 Hz, 2H, Ar*H*), 7.14 – 6.90 (m, 7H, Ar*H*), 6.90 – 6.72 (m, 4H, Ar*H*), 6.71 – 6.54 (m, 3H, Ar*H*), 2.33 (s, 3H, NiCOCH_3), 1.96 – 1.77 (m, 6H,*o*-PhCH_3), 1.59 – 1.48 (m, 2H, PC*H*(CH_3)$_2$), 0.86 (dd, *J* = 16.6, 7.0 Hz, 3H, PCH(CH_3)$_2$), 0.60 (dd, *J* = 17.5, 7.0 Hz, 3H, PCH(CH_3)$_2$), 0.43 (dd, *J* = 14.9, 7.0 Hz, 3H, PCH(CH_3)$_2$), 0.22 (dd, *J* = 18.3, 7.2 Hz, 3H, PCH(CH_3)$_2$). ^{31}P{^{1}H} NMR (121 MHz, C_6D_6): δ (ppm) 59.3, 33.7. ^{19}F NMR (282 MHz, C_6D_6): δ (ppm) -142.8 (m), -147.2 (m).

X-ray crystallographic studies. The single crystal of **5d**•CO was obtained by keeping a diethyl ether solution of **5d** under 1 atm of CO at -25 °C. The single crystal of co-crystallized **5d** and **5d**•CO was obtained by slow diffusion of hexane layered on tope of a toluene solution of **5d** under 1 atm of CO at -25 °C.

X-ray intensity data were measured on a Bruker CCD-based diffractometer with dual Cu/Mo ImuS microfocus optics (Cu Kα radiation, λ = 1.54178 A, Mo Kα radiation, λ =0.71073 A). MO radiation was used for **5d•CO** and Cu radiation was used for the co-crystal of **5d** and **5d•CO**. A crystal was mounted on a cryoloop using Paratone oil and placed under a steam of nitrogen at 100 K (Oxford Cryosystems). The data was corrected for absorption with the SADABS program. The structures were refined using the Bruker SHELXTL Software Package (Version 6.1) and were solved using direct methods until the final anisotropic full matrix, least squares refinement of F2 converged. CCDC 2092650 and 2092911 contain the supplementary crystallographic data for this paper. The data can be obtained free of charge from The Cambridge Crystallographic Data Centre via www.ccdc.cam.ac.uk/structures.

High-Pressure IR Study. A Mettler Toledo ReactIR 702 spectrometer with a SiComp high-pressure probe was used to record the IR spectra at various pressures. In a typical experiment, an autoclave with the SiComp probe attached to its bottom was evacuated overnight before use. A pure solvent (dichloromethane or toluene, 3 mL) was added via the injection port into the autoclave to cover the SiComp probe. The Mettler Toledo ReactIR 702 spectrometer was connected to the SiComp probe via an optical fiber conduit. The solvent background was collected. Then, a solution of **5** in 5 mL of the solvent was injected into the reactor. The reactor was pressurized to a desired CO pressure, and the IR data were collected. The final spectrum was generated after subtraction of the background (see Supporting Information for the IR spectra of **5d** as representative examples). The wavenumbers of the acetyl C=O stretching vibrations are summarized in Table 3.

Table 3. The acetyl C=O stretching vibration wavenumbers ($\nu_{C=O}$) of zwitterionic Ni(II) compounds.

compound	**5a**	**5a**•CO	**5b**	**5b**•CO	**5c**	**5c**•CO	**5d**	**5d**•CO	**5e**	**5e**•CO	**5f**	**5f**•CO
$\nu_{C=O}$ (cm^{-1})	1692	1715	1691	1710	1679	1704	1688	1708	1687	1706	1684	1712

Determination of equilibrium constants. Since the C=O stretching vibrations of **5** and **5**•CO (Table 3) presumably have different absorptivities, the [**5**]/[**5•CO**] ratio cannot be directly quantified by the intensity of these absorptions. Consequently, the equilibrium constants are determined using methods described below in three different scenarios.

For **5a**, **5b** and **5f**, **5** and **5**•CO (eq 1, Table 2) were present under 1 atm of CO, but **6** was not. K_1 was estimated to be < 0.1 but not determined. Under 60 atm of CO, **5**•CO became the only observable Ni species in IR. An approximation was taken to determine K_2: $h_{tot} = A[\mathrm{Ni}]_{tot} \approx A[\mathbf{5}\text{•CO}]_{60atm}$, where h_{tot} is the height of $\nu_{C=O}$ of **5**•CO when **5**•CO is the only Ni species present in the solution, A is the absorptivity of $\nu_{C=O}$ of **5**•CO; and [**Ni**]$_{tot}$ is the total molar concentration of Ni charged into the autoclave. Upon lowing CO pressure to P, some **5**•CO is converted to **5**; $[\mathrm{Ni}]_{\mathrm{total}} - [\mathbf{5}\bullet\mathrm{CO}]_{\mathrm{p}} = [\mathbf{5}]_{\mathrm{p}}$. Therefore, we have $h_{\mathrm{tot}} - h_{\mathrm{p}} = A[\mathrm{Ni}]_{\mathrm{total}} - A[\mathbf{5}\bullet\mathrm{CO}]_{\mathrm{p}} = A[\mathbf{5}]_{\mathrm{p}}$, where h_{p} is the height of $\nu_{\mathrm{C=O}}$ of **5**•CO at the pressure P. The equilibrium constant is calculated as $K_2 = [\mathbf{5}]_{\mathrm{p}}\mathrm{P}/[\mathbf{5}\bullet\mathrm{CO}]_{\mathrm{p}} = (h_{\mathrm{tot}} - h_{\mathrm{p}})\mathrm{P}/h_{\mathrm{p}}$, with the unit of P being atmosphere. Note that A does not have to be determined as it is cancelled out, but h_{tot} must be measured.

For **5c** and **5e**, **5** (eq 1, Table 2) is the only species observable under 1 atm of CO. Again, K_1 was estimated to be < 0.1 but not determined, and an approximation was taken to determine K_2: $h_{\mathrm{tot}} = A[\mathrm{Ni}]_{\mathrm{tot}} \approx A[\mathbf{5}]_{1\mathrm{atm}}$, where h_{total} is the height of $\nu_{\mathrm{C=O}}$ of **5** when **5** is the only Ni species present in the solution, A is the absorptivity of $\nu_{\mathrm{C=O}}$ of **5**; and $[\mathbf{Ni}]_{\mathrm{tot}}$ is the total molar concentration of Ni charged into the autoclave. Upon increasing CO pressure to P, some **5** is converted to **5•CO**; $[\mathrm{Ni}]_{\mathrm{total}} - [\mathbf{5}]_{\mathrm{p}} = [\mathbf{5}\bullet\mathrm{CO}]_{\mathrm{p}}$, hence $h_{\mathrm{tot}} - h_{\mathrm{p}} = A[\mathrm{Ni}]_{\mathrm{tot}} - A[\mathbf{5}]_{\mathrm{p}} = A[\mathbf{5\bullet CO}]_{\mathrm{p}}$. The equilibrium constant is calculated as $K_2 = [\mathbf{5}]_{\mathrm{p}}\mathrm{P}/[\mathbf{5}\bullet\mathrm{CO}]_{\mathrm{p}} = h_{\mathrm{p}}\mathrm{P}/(h_{\mathrm{tot}} - h_{\mathrm{p}})$.

For **5d**, **5**, **5**•CO, and **6** (eq 1, Table 2) are all substantially present under 1 atm of CO. As in the cases of **5a**, **5b** and **5f**, **5**•CO became the only observable Ni species in IR under 60 atm of CO, and the approximation $[\mathrm{Ni}]_{\mathrm{tot}} \approx [\mathbf{5}\bullet\mathrm{CO}]_{60\mathrm{atm}}$ was taken. Upon lowing CO pressure to 1 atm, the height of $\nu_{\mathrm{C=O}}$ of **5**•CO decreased to $h_{1\mathrm{atm}}$, and $[\mathbf{5}\bullet\mathrm{CO}]_{1\mathrm{atm}}$ can be determined as $[\mathbf{5}\bullet\mathrm{CO}]_{1\mathrm{atm}} = (h_{1\mathrm{atm}}/h_{60\mathrm{atm}})[\mathrm{Ni}]_{\mathrm{tot}}$. From the ^{1}H NMR integration of the acetyl and methyl peaks, the ratio $([\mathbf{5}]_{1\mathrm{atm}} + [\mathbf{5}\bullet\mathrm{CO}]_{1\mathrm{atm}})/[\mathbf{6}]_{1\mathrm{atm}}$ was obtained. From this and $[\mathrm{Ni}]_{\mathrm{total}} = [\mathbf{5}\bullet\mathrm{CO}]_{1\mathrm{atm}} + [\mathbf{5}]_{1\mathrm{atm}} + [\mathbf{6}]_{1\mathrm{atm}}$, $[\mathbf{5}]_{1\mathrm{atm}}$ and $[\mathbf{6}]_{1\mathrm{atm}}$ were solved. The values of K_1 and K_2 were calculated from the concentrations under 1 atm.

Polymerization Procedure. A catalyst (15 mg) was charged in a Parr high-pressure reactor in a glovebox. The reactor was connected to a Schlenk line and exposed to 1 atm of CO in a well-ventilated fume food. Under a steady flow of CO, the solvent was injected into the reactor. Next, the reactor was pressurized with ethylene and CO (300 psi each). The reaction mixture was stirred with a magnetic stirrer, and the polymerization was stopped by releasing the pressure after a period of time specified in Table 1S (see Supporting Information). The polyketone product was isolated after filtration and removal of the residual solvent under vacuum.

ASSOCIATED CONTENT

Supporting Information

The supporting information is available free of charge on ACS publication website at DOI:
X-rays crystallographic data for **5d**•CO and a co-crystal of **5d** and **5d**•CO (CIF, CCDC 2092911 and 2092650), NMR spectra, IR spectra, and Zimm plots of light scattering measurements.

AUTHOR INFORMATION

Corresponding Author

* E-mail for Li Jia: ljia@uakron.edu.

Notes

The authors declare no competing financial interest.

ACKNOWLEDGMENT

The research is supported by the National Science Foundation of USA (CHE-1900430).

References

1. Sen, A., Mechanistic aspects of metal-catalyzed alternating copolymerization of olefins with carbon monoxide. *Accounts of Chemical Research* **2002,** *26*, 303-310.
2. Brule, E.; Guo, J.; Coates, G. W.; Thomas, C. M., Metal-catalyzed synthesis of alternating copolymers. *Macromol. Rapid Commun.* **2011,** *32*, 169-85.
3. Drent, E.; Budzelaar, P. H., Palladium-Catalyzed Alternating Copolymerization of Alkenes and Carbon Monoxide. *Chem Rev* **1996,** *96*, 663-682.
4. Zong, Y. L.; Li, Q. K.; Mu, H. L.; Jian, Z. B., Palladium Promoted Copolymerization of Carbon Monoxide with Polar or Non-polar Olefinic Monomers. *Curr. Org. Chem.* **2021,** *25*, 287-300.
5. Sommazzi, A.; Garbassi, F., Olefin carbon monoxide copolymers. *Prog. Polym. Sci.* **1997,** *22*, 1547-1605.
6. Daglen, B. C.; Tyler, D. R., Photodegradable plastics: end-of-life design principles. *Green Chemistry Letters and Reviews* **2010,** *3*, 69-82.
7. Bianchini, C.; Meli, A., Alternating copolymerization of carbon monoxide and olefins by single-site metal catalysis. *Coord. Chem. Rev.* **2002,** *225*, 35-66.
8. Leone, A.; Consiglio, G., Copolymerization of Ethene and Carbon Monoxide with (Diphosphine)nickel Catalysts. *Helvetica Chimica Acta* **2006,** *89*, 2720-2727.
9. Drent, E. Catalytic preparation of polyketone from carbon monoxide and olefin. U.S. Patent 4835250. 1989.
10. Drent, E.; De Kock, M. C. T. Catalyst composition and process for the preparation of copolymers of carbon monoxide and an olefinically unsaturated compound. U.S. Patent 5688909. 1997.
11. Jan Karel Frederik Buijink; Eit Drent; Suykerbuyk, J. C. L. J. Catalyst composition and process for the preparation of copolymers of carbon monoxide and an olefinically unsaturated compound. WO Patent 2000009584. 2000.
12. Klabunde, U.; Itten, S. D., Nickel catalysis for ethylene homo- and co-polymerization. *J. Mol. Catal.* **1987,** *41*, 123-134.
13. Klabunde, U.; Tulip, T. H.; Roe, D. C.; Ittel, S. D., Reaction of nickel polymerization catalysts with carbon monoxide. *J. Organomet. Chem.* **1987,** *334*, 141-156.
14. Beckmann, U.; Eichberger, E.; Rufińska, A.; Sablong, R.; Kläui, W., Nickel(II) catalysed co-polymerisation of CO and ethene: Formation of polyketone vs. polyethylene – The role of co-catalysts. *J. Catal.* **2011,** *283*, 143-148.
15. Kläui, W.; Bongards, J.; J. Reiß, G., Novel Nickel(II) Complexes for the Catalytic Copolymerization of Ethylene and Carbon Monoxide: Polyketone Synthesis in Supercritical Carbon Dioxide. *Angew. Chem.* **2000,** *39*, 3894-3896.
16. Roukoss, C.; Fiddy, S.; de Mallmann, A.; Rendon, N.; Basset, J. M.; Kuntz, E.; Coperet, C., Access to well-defined isolated Fe(II) centers on silica and their use in oxidation. *Dalton Trans* **2007**, 5546-8.
17. Drent, E.; van Dijk, R.; van Ginkel, R.; van Oort, B.; Pugh, R. I., The first example of palladium catalysed non-perfectly alternating copolymerisation of ethene and carbon monoxide. *Chem Commun (Camb)* **2002**, 964-5.
18. Haras, A.; Michalak, A.; Rieger, B.; Ziegler, T., Theoretical analysis of factors controlling the nonalternating CO/C(2)H(4) copolymerization. *J Am Chem Soc* **2005,** *127*, 8765-74.
19. Soomro, S. S.; Cozzula, D.; Leitner, W.; Vogt, H.; Muller, T. E., The microstructure and melt properties of CO-ethylene copolymers with remarkably low CO content. *Polymer Chemistry* **2014,** *5*, 3831-3837.

20. Chen, C.; Anselment, T. M. J.; Frohlich, R.; Rieger, B.; Kehr, G.; Erker, G., o-Diarylphosphinoferrocene Sulfonate Palladium Systems for Nonalternating Ethene-Carbon Monoxide Copolymerization. *Organometallics* **2011,** *30*, 5248-5257.
21. Hearley, A. K.; Nowack, R. A. J.; Rieger, B., New single-site palladium catalysts for the nonalternating copolymerization of ethylene and carbon monoxide. *Organometallics* **2005,** *24*, 2755-2763.
22. Newsham, D. K.; Borkar, S.; Sen, A.; Conner, D. M.; Goodall, B. L., Inhibitory Role of Carbon Monoxide in Palladium(II)-Catalyzed Nonalternating Ethene/Carbon Monoxide Copolymerizations and the Synthesis of Polyethene-block-poly(ethene-alt-carbon monoxide). *Organometallics* **2007,** *26*, 3636-3638.
23. Luo, R.; Newsham, D. K.; Sen, A., Palladium-Catalyzed Nonalternating Copolymerization of Ethene and Carbon Monoxide: Scope and Mechanism. *Organometallics* **2009,** *28*, 6994-7000.
24. Chen, S. Y.; Pan, R. C.; Chen, M.; Liu, Y.; Chen, C.; Lu, X. B., Synthesis of Nonalternating Polyketones Using Cationic Diphosphazane Monoxide-Palladium Complexes. *J. Am. Chem. Soc.* **2021,** *143*, 10743-10750.
25. Thomas, J. C.; Peters, J. C., Benzene C-H activation at a charge neutral zwitterionic platinum(II) complex. *J. Am. Chem. Soc.* **2001,** *123*, 5100-1.
26. Thomas, C. M.; Peters, J. C., Coordinating anions: (phosphino)tetraphenylborate ligands as new reagents for synthesis. *Inorg. Chem.* **2004,** *43*, 8-10.
27. Tassone, J. P.; Mawhinney, R. C.; Spivak, G. J., An examination of the effects of borate group proximity on phosphine donor power in anionic (phosphino)tetraphenylborate ligands. *J. Organomet. Chem.* **2015,** *776*, 153-156.
28. Peters, J. C.; Feldman, J. D.; Tilley, T. D., Silylene Extrusion from a Silane: Direct Conversion of Mes2SiH2 to an Iridium Silylene Dihydride. *J. Am. Chem. Soc.* **1999,** *121*, 9871-9872.
29. Lavallo, V.; Wright, J. H., 2nd; Tham, F. S.; Quinlivan, S., Perhalogenated carba-closo-dodecaborate anions as ligand substituents: applications in gold catalysis. *Angew. Chem. Int. Ed. Engl.* **2013,** *52*, 3172-6.
30. Konishi, S.; Iwai, T.; Sawamura, M., Synthesis, Properties, and Catalytic Application of a Triptycene-Type Borate-Phosphine Ligand. *Organometallics* **2018,** *37*, 1876-1883.
31. Kim, Y.; Jordan, R. F., Synthesis, Structures, and Ethylene Dimerization Reactivity of Palladium Alkyl Complexes That Contain a Chelating Phosphine-Trifluoroborate Ligand. *Organometallics* **2011,** *30*, 4250-4256.
32. Jaska, C. A.; Dorn, H.; Lough, A. J.; Manners, I., Chemistry of phosphine-borane adducts at platinum centers: synthesis and reactivity of PtII complexes with phosphinoborane ligands. *Chemistry* **2003,** *9*, 271-81.
33. Hoic, D. A.; Davis, W. M.; Fu, G. C., Diphenylphosphidoboratabenzene: An Anionic Analogue of Triphenylphosphine. *J. Am. Chem. Soc.* **1996,** *118*, 8176-8177.
34. Granville, S. L.; Welch, G. C.; Stephan, D. W., Ni, Pd, Pt, and Ru complexes of phosphine-borate ligands. *Inorg. Chem.* **2012,** *51*, 4711-21.
35. Fischbach, A.; Bazinet, P. R.; Waterman, R.; Tilley, T. D., β-Phosphinoethylboranes as Ambiphilic Ligands in Nickel−Methyl Complexes. *Organometallics* **2008,** *27*, 1135-1139.
36. Drover, M. W.; Nagata, K.; Peters, J. C., Fusing triphenylphosphine with tetraphenylborate: introducing the 9-phosphatriptycene-10-phenylborate (PTB) anion. *Chem Commun (Camb)* **2018,** *54*, 7916-7919.
37. Barney, A. A.; Heyduk, A. F.; Nocera, D. G., Synthesis of an anionic tridentate phosphinoborate and its reaction chemistry with Sn(II). *Chem. Commun.* **1999**, 2379-2380.
38. Jia, X. F.; Zhang, M. R.; Pan, F.; Babahan, I.; Ding, K. L.; Jia, L.; Crandall, L. A.; Ziegler, C. J., Zwitterionic Nickel(II) Catalyst for CO-Ethylene Alternating Copolymerization. *Organometallics* **2015,** *34*, 4798-4801.

39. Jia, X. F.; Zhang, M. R.; Li, M. H.; Pan, F.; Ding, K. L.; Jia, L.; Crandall, L. A.; Engle, J. T.; Ziegler, C. J., Zwitterionic Nickel(II) Catalysts for CO-Ethylene Alternating Copolymerization. *Organometallics* **2017,** *36*, 1122-1132.
40. Dai, Y.; He, S.; Peng, B.; Crandall, L. A.; Schrage, B. R.; Ziegler, C. J.; Jia, L., Zwitterionic Design Principle of Nickel(II) Catalysts for Carbonylative Polymerization of Cyclic Ethers. *Angew Chem Int Ed Engl* **2018,** *57*, 14111-14115.
41. Wax, M. J.; Bergman, R. G. J. J. o. t. A. C. S., Direct evidence for solvent coordination in migratory carbon monoxide insertion. **1981,** *103*, 7028-7030.
42. Vavasori, A.; Ronchin, L., Polyketones: Synthesis and Applications. In *Encyclopedia of Polymer Science and Technology*,2017; pp 1-41.
43. Gordon, M.; Roe, R.-J. J. P., Surface-chemical mechanism of heterogeneous polymerization and derivation of Tung's and Wesslau's molecular weight distribution. **1961,** *2*, 41-59.